*Systematic Review*

# Evaluating Different Quantitative Shear Wave Parameters of Ultrasound Elastography in the Diagnosis of Lymph Node Malignancies: A Systematic Review and Meta-Analysis

Yujia Gao [1,*], Yi Zhao [2], Sunyoung Choi [3], Anjalee Chaurasia [2], Hao Ding [2], Athar Haroon [4], Simon Wan [5] and Sola Adeleke [6,7]

1   UCL Medical School, University College London, London WC1E 6BT, UK
2   Imperial College London, School of Medicine, London SW7 2DD, UK
3   GKT School of Medicine, King's College London, London WC2R 2LS, UK
4   Department of Nuclear Medicine, Barts Health NHS Trust, London E1 1BB, UK
5   Institute of Nuclear Medicine, University College London, London NW1 2BU, UK
6   Department of Oncology, Guy's and St Thomas' NHS Foundation Trust, London SE1 9RT, UK
7   School of Cancer & Pharmaceutical Sciences, King's College London, London WC2R 2LS, UK
*   Correspondence: yujia.gao.19@ucl.ac.uk

**Simple Summary:** Ultrasound (US) imaging is a safe, convenient imaging method for identifying malignant lymph nodes. Shear wave elastography (SWE), as a type of US elastography offers the mechanical information of tissue by sensing shear wave propagation in lymph nodes. Malignant lymph nodes can show increased stiffness at the lesion margin and adjacent tissue on the SWE image. However, the diagnostic accuracies of various SWE parameters that quantify tissue stiffness, such as maximum stiffness, mean stiffness, minimum stiffness, and standard deviation, are yet to be demonstrated. We included sixteen eligible studies to evaluate the pooled diagnostic accuracy of different SWE parameters. SWE has demonstrated promise as an imaging modality in diagnosing and differentiating malignancy from benign lymph nodes. Its incorporation into standard US allows for a better evaluation of the target region or lymph node and might reduce the need for invasive procedures or exposure to ionising radiation without compromising on diagnostic accuracy.

**Abstract:** Shear wave elastography (SWE) has shown promise in distinguishing lymph node malignancies. However, the diagnostic accuracies of various SWE parameters that quantify tissue stiffness are yet to be demonstrated. To evaluate the pooled diagnostic accuracy of different SWE parameters for differentiating lymph node malignancies, we conducted a systematic screening of four databases using the PRISMA guidelines. Lymph node biopsy was adopted as the reference standard. $E_{max}$ (maximum stiffness), $E_{mean}$ (mean stiffness), $E_{min}$ (minimum stiffness), and $E_{sd}$ (standard deviation) SWE parameters were subjected to separate meta-analyses. A sub-group analysis comparing the use of $E_{max}$ in cervical (including thyroid) and axillary lymph node malignancies was also conducted. Sixteen studies were included in this meta-analysis. $E_{max}$ and $E_{sd}$ demonstrated the highest pooled sensitivity (0.78 (95% CI: 0.69–0.87); 0.78 (95% CI: 0.68–0.87)), while $E_{mean}$ demonstrated the highest pooled specificity (0.93 (95% CI: 0.88–0.98)). From the sub-group analysis, the diagnostic performance did not differ significantly in cervical and axillary LN malignancies. In conclusion, SWE is a promising adjunct imaging technique to conventional ultrasonography in the diagnosis of lymph node malignancy. SWE parameters of $E_{max}$ and $E_{sd}$ have been identified as better choices of parameters for screening clinical purposes.

**Keywords:** elastography; shear wave elastography (SWE); lymph node malignancy; lymphoma; ultrasound elastography

## 1. Introduction

Lymph node (LN) analysis is commonly used for assessing cancer recurrences, metastases, and pre-treatment cancer TNM staging [1]. The abnormal change in LN size, consistency and number is associated with either benign or malignant pathological phenomena [2–4]. For example, painless hardened LNs are frequently indicators of metastatic cancer or granulomatous diseases, whereas firm and rubbery LNs may indicate lymphoma [5]. Nodal status assessment is essential in patients with known cancer malignancies as it helps tailor treatment options, decision-making, and predicting prognosis [6]. Therefore, the accurate identification of the nature of lymphadenopathy is crucial yet clinically difficult due to the problems in differentiating malignant lesions from benign ones [7].

Ultrasound (US) imaging is a common complementary imaging modality for the evaluation of lymph nodes due to its safety, convenience, and relative low costs [8]. Sonographic features, such as cystic transformation, microcalcification, hyperechogenicity, or aberrant vascularity, have been linked to LN malignancy. However, no single US reporting standard for identifying malignant LNs with satisfactory sensitivity and specificity has been developed [9,10].

The newly emerged technique, US elastography, first proposed by Ophir et al [4], offers mechanical information of tissue by sensing internal tissue deformation or displacement in response to an applied force and displays the resulting information in a suitable form [11]. Since malignant LNs are frequently infiltrated by tumour cells, tumoral necrosis, and calcification but benign LNs are not, the stiffness difference between malignant and benign LNs can provide important clinical information to differentiate LN states [12]. Similar to standard ultrasound imaging, US elastography overcomes the limitations of manual examination, for example limited accessibility to organs, subjective interpretation, and inaccurate disease localization [13,14]. In addition, it provides information on lesions that may not have sonographic contrast that otherwise could have been detected ultrasonically [15]. Several studies have documented the utility of US elastography in differentiating malignant from benign lesions in breast, thyroid, prostate, and liver, as well as lymph nodes [8,16–20], and encouraging findings with higher diagnostic accuracy than B-mode in standard ultrasound [21,22] or as an adjunct technique have been observed [16,23].

Depending on the type of force applied, either quasi-static (probe palpation or compression) or dynamic (thumping or vibrating), US elastography could examine the tissue deformation in two ways: strain elastography (SE), which measures tissue strain, or shear wave elastography (SWE) measuring shear wave propagation [11,24]. The current literature associates SWE to methods visualising shear-wave speed using acoustic radiation force [11], including both two-dimensional and three-dimensional SWE. Transverse orientated shear waves are generated and propagated through target tissues with varying elasticities at different velocities [25]. The final elasticity can be directly and qualitatively interpreted via a colour map overlaid on the B-mode ultrasonic image or through conversion into Young's modulus, in kilopascals (kPa), for quantitative analysis within a region of interest [18,26,27]. The qualitative analysis of SWE classifies elastograms into various colour patterns [28]; however, the number of patterns comparably vary between study groups hampering the results. Malignant lymph nodes can show the stiff rim sign: increased stiffness at the lesion margin and adjacent tissue on the elastogram. The region of interest (ROI) is set over the stiffest part of the immediate adjacent stiff tissue, and the abnormal lymph nodes can be quantified using shear wave values [29].

The current literature reports different quantitative SWE parameters: $E_{min}$ (minimum stiffness), $E_{mean}$ (mean stiffness), $E_{max}$ (maximum stiffness), and $E_{sd}$ (one standard deviation of stiffness) with different cut-off values for different anatomical lymph node positions [12,16,19,22,29–35]. However, more evidence is needed to discuss the significance of the different SWE parameters and their diagnostic potential for lymph node diseases. The aim of this study is to investigate the role of SWE parameters as potential predictive parameters in lymph node malignancies and to evaluate their diagnostic accuracy for the differentiation between benign and malignant lymph nodes.

## 2. Materials and Methods

### 2.1. Literature Search

A systematic search was carried out using Medline, Ovid, PubMed, Embase, and Web of Science databases to retrieve all studies that contribute relevant evidence from inception to date. The search included Medical Subject Heading (MeSH) terms and free text with appropriate Boolean operators. The following terms were included in the search: "shear wave elastography", "elastography", "lymph node OR lymph gland", and "diagnosis", as well as multiple synonyms, were used to account for differences in terminology. In the case of absent or ambiguous data, the corresponding authors were contacted directly for clarification.

Eligible studies were screened independently by two researchers (Y. Gao and Y. Zhao). Articles considered eligible had the full text in English retrieved for further review. Any disagreements between reviewers were discussed until a consensus was reached, and in cases where this was not possible, a third case reviewer was consulted. The study was designed using the PRISMA-P (Preferred Reporting Items for Systematic Reviews and Meta-analysis Protocols) and was registered with PROSPERO (CRD42022322053). All exclusions were noted for further analysis and the reasons were documented in detail to generate the PRISMA flow (Figure 1 ) [36]. We continued updating the literature search until August 2022 and the bibliographies of articles were also screened to identify all appropriate articles.
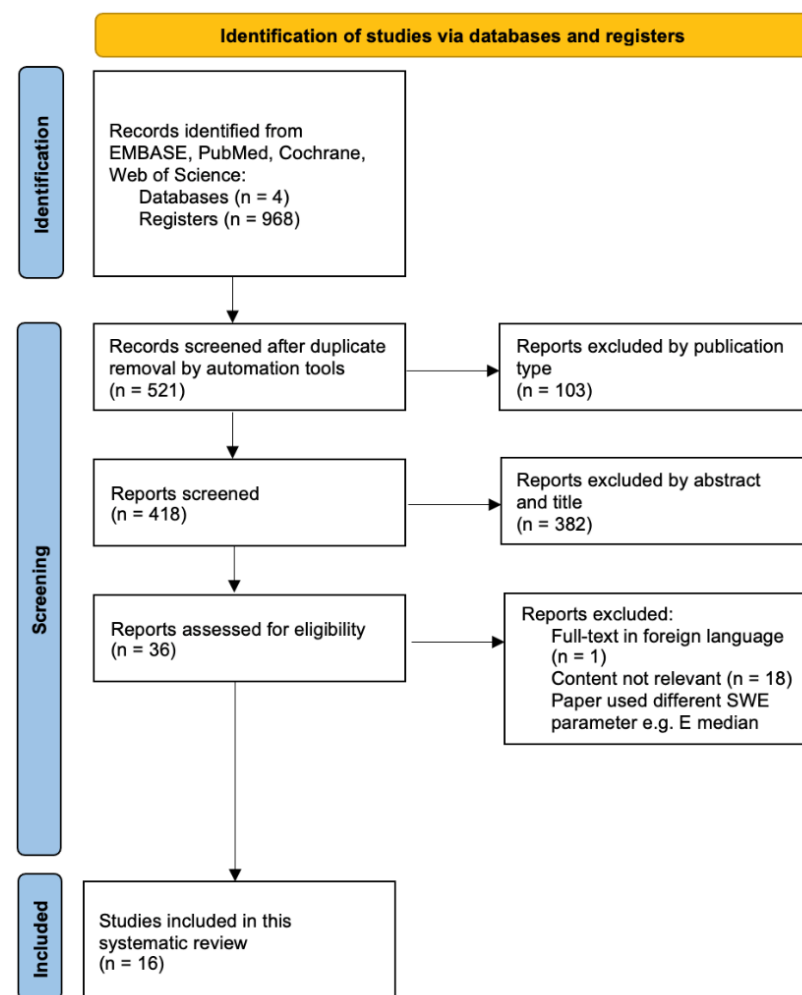


**Figure 1.** PRISMA flow diagram of evidence acquisition.

Search terms used are: (((((elastography OR strain elastography OR real time elastography OR shear wave elastography) AND (lymph node OR lymph gland OR disease)) AND Meta*) AND Diagno*) AND Accurac*). ti,ab.

### 2.2. Data Collection

All desired data were collected and summarised in a dedicated datasheet (Table 1). Study characteristics, such as authors, year of publication and study design, and the demographics of patient population, patient mean age, number of lymph node lesions, and the lymph node type, were noted. Information from study methodology and outcomes, including SWE imaging strength, SWE parameters/settings, elasticity cut-off values, and mean elasticity value in lymph node malignancy, as well as histopathology methods and definition for clinically significant disease, were reported.

### 2.3. Inclusion Criteria

Studies which included patients who received shear wave elastography with underlying pathology of lymph node malignancies were considered eligible for inclusion. Studies fulfilling the following requirements were included in the meta-analysis: (1) the study was published in English with accessible full text; (2) shear wave ultrasound elastography was used to assess lymph node status; (3) study design was observational, either prospective or retrospective; (4) the study has used reference standards that was based on histopathology reports, biopsy, or fine needle aspiration; (5) the study contained full set of clinical data that could be directly or indirectly obtained, including true positives, true negatives, false positives, false negatives, sensitivity, specificity, PPV, and NPV to construct diagnostic tables.

### 2.4. Exclusion Criteria

Studies matching the following criteria were excluded: (1) studies there were on topics other than using the value of elasticity modulus (kPa) to diagnose lymph node malignancies; (2) studies that were not using shear wave elastography but strain elastography; (3) studies that were not performed to differentiate lymph node malignancies; (4) studies that were correspondence articles, expert opinions, conference abstracts, review articles and case reports, or not original papers; and (5) studies with text in a foreign language besides English.

**Table 1.** Study characteristics of included studies.

| Authors | Year of Publication | Study Design | No. of Patients | Mean Age (Range) (Years Old) | No. of Lymph Node Lesions | US Imaging System | SWE Imaging Strength (MHz) | SWE Parameters | Elastic Modulus Values in Malignant Lymph Nodes Mean $\pm$ SD or Median (IQR) (kPa) | LN Type | Reference Standard | Clinically Significant Definition |
|---|---|---|---|---|---|---|---|---|---|---|---|---|
| Ng et al. [16] | 2022 | Prospective | 107 | 58 (32–82) | 107 | Aixplorer (SuperSonic Imagine) | 15-4 | $E_{max}$ $E_{mean}$ $E_{min}$ $E_{sd}$ | 40.0 $\pm$ 46.4 28.9 $\pm$ 36.4 22.5 $\pm$ 33.5 8.7 $\pm$ 27.1 | Axillary | ALND or SLNB | Bloom and Richardson Grading ALN pathological staging: cut-off point of >3 mm |
| Chami et al. [37] | 2021 | Prospective | 222 | N/A | 222 | Aixplorer (SuperSonic Imagine Ltd, Aix-en-Provence, France) | SL10-2 (central frequency at 10 MHz) | $E_{max}$ $E_{mean}$ $E_{sd}$ | 36.1 $\pm$ 33.7 (lymphoma) 62 $\pm$ 58.2 (carcinoma) 16.7 $\pm$ 12.3 (lymphoma) 29.5 $\pm$ 32.3 (carcinoma) 6.4 $\pm$ 5.7 (lymphoma) 11.1 $\pm$ 10.6 (carcinoma) | Axillary, Head & Neck, Inguinal | CNB | Doppler criteria |
| Yang et al. [32] | 2021 | Retrospective | 103 | 43.9 (18–66) | 109 | Aixplorer (SuperSonic Imagine, Aixen-Provence, France) | 15-4 | $E_{max}$ | 34.2 $\pm$ 7.0 | Cervical | US-guided biopsy | US criterion; transverse diameter of >7 mm (level II–VI), peripheral/mixed blood flow present |
| Lo et al. [38] | 2019 | Prospective | 109 | 46 (21–86) | 109 | Toshiba Aplio 500 US system (Otawara, Japan) | 15-4 | $E_{max}$ | 66.3 $\pm$ 24.3 | Cervical | US-FNA or US-CNB | - |
| Luo et al. [31] | 2019 | Prospective | 118 | 46.7 (27–69) | 121 | Aixplorer ultrasound system (Supersonic Imagine, Aix-en-Provence, France) | 15-4 | $E_{max}$ $E_{mean}$ $E_{min}$ $E_{sd}$ | 54.79 $\pm$ 37.42 49.93 $\pm$ 35.68 41.88 $\pm$ 32.67 3.74 $\pm$ 3.16 | Axillary | ALNB or SLNB | Tumour deposit > 0.2 mm in diameter in at least one lymph node |
| Chen et al. [34] | 2018 | Prospective | 62 | 43.5 (19–66) | 114 | Aixplorer (SuperSonic Imagine, Aixen-Provence, France) | 15-4 | $E_{max}$ $E_{mean}$ $E_{min}$ | 31.6 (IQR: 25.2; 55.9) 22.4 (IQR: 18.8; 36.6) 15.8 (IQR: 9.6; 22.4) | Cervical | US-Guided CNB | AJCC staging system |
| Kim et al. [30] | 2018 | Retrospective | 43 | 49 (29–81) | 43 | Aixplorer (SuperSonic Imagine, Aix-en-Provence, France) | 15-4 | $E_{max}$ $E_{mean}$ $E_{min}$ $E_{sd}$ | 50.5 (IQR: 39.9; 88.0) 37.1 (IQR: 20.0; 46.3) 11.3 (IQR: 4.2; 34.7) 7.8 (IQR: 4.6; 11.2) | Cervical | FNAB | - |

**Table 1.** *Cont.*

| Authors | Year of Publication | Study Design | No. of Patients | Mean Age (Range) (Years Old) | No. of Lymph Node Lesions | US Imaging System | SWE Imaging Strength (MHz) | SWE Parameters | Elastic Modulus Values in Malignant Lymph Nodes Mean $\pm$ SD or Median (IQR) (kPa) | LN Type | Reference Standard | Clinically Significant Definition |
|---|---|---|---|---|---|---|---|---|---|---|---|---|
| Seo et al. [29] | 2018 | Retrospective | 53 | 54.7 (33–80) * | 54 | Aixplorer (Supersonic Imagine, Aix en Provence, France) | 15-4 | $E_{max}$ $E_{mean}$ $E_{min}$ $E_{sd}$ | 79.80 $\pm$ 65.95 55.99 $\pm$ 49.19 29.29 $\pm$ 31.44 13.92 $\pm$ 11.46 | Axillary | US-guided FNAB or SLNB | US criterion |
| You et al. [39] | 2018 | Prospective | 39 | 45.6 (15–67) | 141 | Aixplorer US system (SuperSonic Imagine, Aix en Provence, France) | 15-4 | $E_{max}$ $E_{mean}$ $E_{min}$ $E_{sd}$ | 58.7 $\pm$ 25.7 30.6 $\pm$ 14.9 11.9 $\pm$ 9.1 10.2 $\pm$ 5.0 | Cervical | FNAB | US criterion 18 months follow-up |
| Tan et al. [40] | 2017 | Prospective | 42 | 44 (23–61) | 42 | Aixplorer US system (SuperSonic Imagine, Aix-en-Provence, France) | SL10-2 | $E_{max}$ $E_{mean}$ $E_{min}$ $E_{sd}$ | 52.0 (IQR: 38.1; 65.1) 16.8 (IQR: 10.6; 26.1) 0.1 (IQR: 0.1; 0.4) 9.1 (IQR: 6.9; 11.7) | Neck, Supra-clavicular fossze, axilla | CNB | NA |
| Youk et al. [22] | 2017 | Retrospective | 130 | 49.4 (18–84) | 130 | Aixplorer (SuperSonic Imagine, Aix-en-Provence, France) | 15-4 | $E_{max}$ $E_{mean}$ $E_{min}$ $E_{sd}$ | 64.6 $\pm$ 41.9 50.2 $\pm$ 31.8 31.4 $\pm$ 24.8 9.0 $\pm$ 9.7 | Axillary | ALND and SLNB | - |
| Desmots et al. [41] | 2016 | Prospective | 56 | 49 (25–84) | 63 (62 involved in further analysis) | Aixplorer, SuperSonic Imagine, Aix-en-Provence, France) with a conventional 15- to 4-MHz transducer linear probe (SuperLinear SL15-4) | SL15–4 | $E_{max}$ | 72 $\pm$ 59 | Head & Neck | Surgical resection, FNAC and US-follow up | AJCC staging system |
| Jung et al. [19] | 2015 | Retrospective | 66 | 45.2 | 84 | Aixplorer (SuperSonic Imagine, Les Jardins de la Duranne, Aix en Provence, France) | 15-4 | $E_{max}$ | 79.61 $\pm$ 71.23 | Cervical | US-Guided FNAB | US criterion |
| Choi et al. [35] | 2013 | Prospective | 15 | 54.2 (38–73) | 67 | Aixplorer (SuperSonic Imagine, Aix en Provence, France) | 15-4 | $E_{max}$ $E_{mean}$ $E_{min}$ | 67.93 $\pm$ 62.52 48.49 $\pm$ 47.21 41.06 $\pm$ 36.34 | Cervical | Surgical resection | US criterion |

**Table 1.** *Cont.*

| Authors | Year of Publication | Study Design | No. of Patients | Mean Age (Range) (Years Old) | No. of Lymph Node Lesions | US Imaging System | SWE Imaging Strength (MHz) | SWE Parameters | Elastic Modulus Values in Malignant Lymph Nodes Mean ± SD or Median (IQR) (kPa) | LN Type | Reference Standard | Clinically Significant Definition |
|---|---|---|---|---|---|---|---|---|---|---|---|---|
| Bhatia et al. [12] | 2012 | Prospective | 46 | 52.8 (7–74) | 55 | Aixplorer; (SuperSonic Imagine, Les Jardins de la Duranne, Aix en Provence, France) | 15-4 | $E_{max}$ | 42.2 (IQR: 28.5; 126.4) | Cervical | US-Guided FNAB | Doppler criteria |
| | | | | | | | | $E_{mean}$ | 25.0 kPa (IQR: 19.3; 86.2) | | | |
| Tourasse et al. [33] | 2012 | Prospective | 65 | - | 81 | SuperSonic Imagine device (Aix en Provence, France) | N/A | $E_{max}$ | 6.71–44.18 (mean = 23.27) | Axillary | SLNB | - |
| | | | | | | | | $E_{mean}$ | 6.24–29.72 (mean = 17.47) | | | |
| | | | | | | | | $E_{sd}$ | 0.3–9.7 (mean = 2.95) | | | |

* mean age calculated for cohort prior to exclusion of patients. abbreviations: CNB: core needle biopsy; ALND: axillary lymph node dissection; ALNB: axillary lymph node biopsy; SLNB: sentinel lymph node biopsy; FNAB: fine needle aspiration biopsy; AJCC: American Joint Committee on Cancer: lesion size > 2 mm, macro-metastasis; 0.2–2.0 mm, micro-metastasis; and <0.2 mm, isolated tumour cells; US: ultrasound; US criterion: at least one of the following criteria: (i) loss of hilar fat, (ii) cortical heterogeneous echogenicity, (iii) echogenic dots (calcification), (iv) a cystic or necrotic area, and (v) long- to short-axis diameter ratio < 2.0. Doppler criteria: abnormality including increased size (short axis diameter ≥ 6 mm), round shape, abnormal parenchymal echogenicity, architecture, and vascularity.

*2.5. Quality Assessment*

Study quality was assessed using the Quality Assessment of Accuracy Studies (QUADAS-2) tool [42]. The QUADAS-2 explored the risk of bias in four key domains: patient selection, index test, reference standard and flow and timing. Additionally, concerns regarding the applicability of these domains to the systematic review were investigated.

*2.6. Endpoints*

The primary endpoint was to identify if there was statistically significant evidence in supporting the use of shear wave elastography in lymph node malignancy diagnosis.

*2.7. Meta-Analysis*

True positives (TPs), true negatives (TNs), false positives (FPs), and false negatives (FNs) were extracted from all selected studies to produce a contingency table based on the histopathology result and SWE parameter used. Pooled quantitative sensitivities and specificities and accuracies were compared using bivariate analysis at a 95% confidence interval (CIs). The summary receiver operating characteristic (SROC) curves were then generated using the area-under-the-curve (AUC) values presented. Heterogeneity and inter-study variation were quantified through $I^2$.

**3. Results**

*3.1. Study Characteristics*

Sixteen studies were considered eligible for further analysis after screening (Table 2) [12,16,19,22,29–35,37–41]. The studies were published between 2012 to 2022. A total of 1276 patients and 1479 lymph node lesions were included for quantitative SWE parameters analysis. Eleven studies were conducted prospectively [12,16,31,33–35,37–41] and five retrospectively [19,22,29,30,32]. Patients' age ranged from 7 to 86 years old. All studies performed histopathology examination using ultrasound-guided fine needle aspiration biopsy (FNAB), core needle biopsy (CNB), surgically resected specimens or axillary lymph node biopsy (ALNB), or sentinel lymph node biopsy (SLNB) as the reference standard to confirm LN malignancy. The $E_{max}$ parameter was analysed in fifteen studies [12,16,19,22,29–35,38–41] eleven studies conducted $E_{mean}$ analysis [12,19,22,29–31,33,34,37,39,40], seven studies conducted $E_{min}$ analysis [19,22,29–31,34,39], and five studies conducted $E_{sd}$ analysis [22,29,30,39,40]. The cut-off values for individual SWE parameters varied considerably across these studies, ranging between 15.2 to 57 kPa for $E_{max}$ [12,16,19,22,29–35,38–41], 15.5 to 30.2 kPa for $E_{mean}$ [12,19,22,29–31,33,34,37,39,40], 11.4 to 24 kPa for $E_{min}$ [19,22,29–31,34,39], and lastly, 2.1 to 6.9 kPa for $E_{sd}$ [22,29,30,39,40]. The elasticity setting on the kPa display scale was between 0–180 kPa across all studies except Chami et al., which qualitatively displayed between 0–100 kPa, with lowest stiffness at 0 kPa represented by dark blue and highest represented by dark red.

*3.2. Risk of Bias*

A total of sixteen studies were reviewed, which observed an overall low risk of bias and high applicability to the review question [12,16,19,22,29–35,37–41] (Table 3). However, four studies were marked as "fair" in terms of overall diagnostic quality. Ng et al. [16] conducted a case-control study and failed to report on the patient identification and recruitment process for the trial. Touresse et al. [33], You et al. [39], and Youk et al. [22] were also classified as "fair", as the studies did not provide an acceptable description of the flow and timing regarding the index test and standard reference test.

**Table 2.** Statistical characteristics of included studies.

| | | SWE Parameter | Cutoff Values | Number of Lymph Node Lesions | Number of Disease Positive Lymph Nodes | TP | FP | TN | FN | Sensitivity | Spec | PPV | NPV | Accuracy | AUC |
|---|---|---|---|---|---|---|---|---|---|---|---|---|---|---|---|
| Ng et al. [16] | 2022 | $E_{max}$ | 15.2 | 107 | 50 | 26 | 25 | 32 | 24 | 0.52 | 0.56 | 0.51 | 0.57 | 0.54 | 0.61 |
| Chami et al. [37] | 2021 | $E_{mean}$ | 15.2 | 222 | 151 | 66 | 12 | 59 | 85 | 0.44 | 0.83 | 0.85 | 0.41 | 0.56 | 0.66 (95% CI: 0.59–0.73) |
| Yang et al. [32] | 2021 | $E_{max}$ | 31.6 | 109 | 66 | 47 | 1 | 24 | 29 | 0.56 | 0.96 | 0.97 | 0.45 | 0.65 | 0.825 (95% CI 0.741–0.891) |
| Lo et al. [38] | 2019 | $E_{max}$ | 42 | 109 | 24 | 20 | 30 | 55 | 4 | 0.83 | 0.65 | 0.40 | 0.93 | 0.69 | 0.688 (0.601–0.775) |
| Luo et al. [31] | 2019 | $E_{max}$ | 26.05 | 121 | 60 | 56 | 7 | 54 | 4 | 0.93 | 0.89 | 0.89 | 0.93 | 0.91 | 0.94 |
| | | $E_{mean}$ | 26.9 | 121 | 60 | 52 | 2 | 59 | 8 | 0.87 | 0.97 | 0.96 | 0.88 | 0.92 | 0.95 |
| | | $E_{min}$ | 22.75 | 121 | 60 | 49 | 6 | 55 | 11 | 0.82 | 0.90 | 0.89 | 0.83 | 0.86 | 0.91 |
| | | $E_{sd}$ | 2.05 | 121 | 60 | 42 | 5 | 56 | 18 | 0.70 | 0.92 | 0.89 | 0.76 | 0.81 | 0.83 |
| Chen et al. [34] | 2018 | $E_{max}$ | 20.6 | 114 | 26 | 26 | 44 | 44 | 0 | 1.00 | 0.50 | 0.37 | 1.00 | 0.61 | 0.82 |
| | | $E_{mean}$ | 18.4 | 114 | 26 | 22 | 15 | 73 | 4 | 0.85 | 0.83 | 0.59 | 0.95 | 0.83 | 0.88 |
| | | $E_{min}$ | 15.5 | 114 | 26 | 14 | 5 | 83 | 12 | 0.54 | 0.94 | 0.74 | 0.87 | 0.85 | 0.80 |
| Kim et al. [30] | 2018 | $E_{max}$ | 37.5 | 43 | 12 | 10 | 1 | 30 | 2 | 0.83 | 0.97 | 0.91 | 0.94 | 0.93 | 0.93 |
| | | $E_{mean}$ | 23 | 43 | 12 | 8 | 1 | 30 | 4 | 0.67 | 0.97 | 0.89 | 0.88 | 0.88 | 0.94 |
| | | $E_{min}$ | 11.7 | 43 | 12 | 6 | 4 | 27 | 6 | 0.50 | 0.87 | 0.60 | 0.82 | 0.77 | 0.70 |
| | | $E_{sd}$ | 6.9 | 43 | 12 | 7 | 1 | 30 | 5 | 0.58 | 0.97 | 0.88 | 0.86 | 0.86 | 0.77 |
| Seo et al. [29] | 2018 | $E_{max}$ | 20.9 | 54 | 34 | 28 | 1 | 19 | 6 | 0.82 | 0.95 | 0.97 | 0.76 | 0.87 | 0.89 |
| | | $E_{mean}$ | 23.8 | 54 | 34 | 26 | 0 | 20 | 8 | 0.76 | 1.00 | 1.00 | 0.71 | 0.85 | 0.88 |
| | | $E_{min}$ | 11.4 | 54 | 34 | 21 | 1 | 19 | 13 | 0.62 | 0.95 | 0.95 | 0.59 | 0.74 | 0.78 |
| | | $E_{sd}$ | 4.05 | 54 | 34 | 26 | 0 | 20 | 8 | 0.76 | 1.00 | 1.00 | 0.71 | 0.85 | 0.88 |
| You et al. [39] | 2018 | $E_{max}$ | 40.2 | 141 | 35 | 28 | 7 | 99 | 7 | 0.80 | 0.93 | 0.80 | 0.93 | 0.90 | 0.92 |
| | | $E_{mean}$ | 22.1 | 141 | 35 | 26 | 12 | 94 | 9 | 0.74 | 0.89 | 0.68 | 0.91 | 0.85 | 0.87 |
| | | $E_{min}$ | 12.4 | 141 | 35 | 19 | 24 | 82 | 16 | 0.54 | 0.77 | 0.44 | 0.84 | 0.72 | 0.61 |
| | | $E_{sd}$ | 4.1 | 141 | 35 | 32 | 23 | 83 | 3 | 0.91 | 0.78 | 0.58 | 0.97 | 0.82 | 0.92 |

**Table 2.** *Cont.*

| | | SWE Parameter | Cutoff Values | Number of Lymph Node Lesions | Number of Disease Positive Lymph Nodes | TP | FP | TN | FN | Sensitivity | Spec | PPV | NPV | Accuracy | AUC |
|---|---|---|---|---|---|---|---|---|---|---|---|---|---|---|---|
| Tan et al. [40] | 2017 | $E_{max}$ | 37.9 | 42 | 34 | 18 | 4 | 16 | 4 | 0.82 | 0.80 | 0.82 | 0.80 | 0.81 | 0.845 (0.701–0.938) |
| | | $E_{mean}$ | 15.5 | 42 | 34 | 14 | 0 | 20 | 8 | 0.64 | 1.00 | 1.00 | 0.71 | 0.81 | 0.732 (0.573–0.857) |
| | | $E_{sd}$ | 6.3 | 42 | 34 | 18 | 6 | 14 | 4 | 0.82 | 0.70 | 0.75 | 0.78 | 0.76 | 0.777 (0.622–0.891) |
| Youk et al. [22] | 2017 | $E_{max}$ | 25.8 | 130 | 65 | 61 | 9 | 56 | 4 | 0.94 | 0.86 | 0.87 | 0.93 | 0.90 | 0.941 (0.885, 0.974) |
| | | $E_{mean}$ | 18.7 | 130 | 65 | 61 | 8 | 57 | 4 | 0.94 | 0.88 | 0.88 | 0.93 | 0.91 | 0.946 (0.892, 0.978) |
| | | $E_{min}$ | 12.3 | 130 | 65 | 56 | 8 | 57 | 9 | 0.86 | 0.88 | 0.88 | 0.86 | 0.87 | 0.915 (0.853, 0.956) |
| | | $E_{sd}$ | 4 | 130 | 65 | 51 | 7 | 58 | 14 | 0.78 | 0.89 | 0.88 | 0.81 | 0.84 | 0.900 (0.835, 0.945) |
| Desmots et al. [41] | 2016 | $E_{max}$ | 31 | 62 | 30 | 26 | 4 | 28 | 4 | 0.87 | 0.88 | 0.87 | 0.88 | 0.87 | 0.903 ± 0.042 |
| Jung et al. [19] | 2015 | $E_{max}$ | 57 | 84 | 51 | 43 | 23 | 10 | 8 | 0.84 | 0.30 | 0.65 | 0.56 | 0.63 | 0.738 (0.633–0.843) |
| | | $E_{mean}$ | 29 | 84 | 51 | 39 | 11 | 22 | 12 | 0.76 | 0.67 | 0.78 | 0.65 | 0.73 | 0.748 (0.644–0.852) |
| | | $E_{min}$ | 24 | 84 | 51 | 13 | 0 | 33 | 38 | 0.25 | 1.00 | 1.00 | 0.46 | 0.55 | 0.737 (0.632–0.842) |
| Choi et al. [35] | 2013 | $E_{max}$ | 19.44 | 67 | 34 | 31 | 1 | 32 | 3 | 0.91 | 0.97 | 0.97 | 0.91 | 0.94 | 0.96 (95% CI: 0.885, 0.993) |
| Bhatia et al. [12] | 2012 | $E_{max}$ | 45 | 55 | 31 | 15 | 2 | 22 | 16 | 0.48 | 0.92 | 0.88 | 0.58 | 0.67 | 0.77 (95% CI 5 0.57–0.83) |
| | | $E_{mean}$ | 30.2 | 55 | 31 | 13 | 0 | 24 | 18 | 0.42 | 1.00 | 1.00 | 0.57 | 0.62 | 0.77 (95% CI 5 0.57–0.83) |
| Tourasse et al. [33] | 2012 | $E_{max}$ | 26.4704 | 81 | 11 | 4 | 0 | 70 | 7 | 0.36 | 1.00 | 1.00 | 0.91 | 0.91 | 0.75 (95% CI: 0.55–0.95) |
| | | $E_{mean}$ | 23.5947 | 81 | 11 | 2 | 0 | 70 | 9 | 0.18 | 1.00 | 1.00 | 0.89 | 0.89 | 0.76 (95% CI: 0.58–0.94) |

**Table 3.** Quality assessment of all included studies.

| Study | Overall Diagnostic Quality | Risk of Bias | | | | Applicability Concerns | | |
|---|---|---|---|---|---|---|---|---|
| | | Patient Selection | Index Test | Reference Standard | Flow and Timing | Patient Selection | Index Test | Reference Standard |
| Ng et al. [16] | Fair | Unclear | Low | Low | Low | Low | Low | Low |
| Chami et al. [37] | Good | Low | Low | Low | Low | Low | Low | Low |
| Yang et al. [32] | Good | Low | Low | Low | Low | Low | Low | Low |
| Lo et al. [38] | Good | Low | Low | Low | Low | Low | Low | Low |
| Luo et al. [31] | Good | Low | Low | Low | Low | Low | Low | Low |
| Chen et al. [34] | Good | Low | Low | Low | Low | Low | Low | Low |
| Kim et al. [30] | Good | Low | Low | Low | Low | Low | Low | Low |
| Seo et al. [29] | Good | Low | Low | Low | Low | Low | Low | Low |
| You et al. [39] | Fair | Low | Low | Low | Unclear | Low | Low | Low |
| Tan et al. [40] | Good | Low | Low | Low | Low | Low | Low | Low |
| Youk et al. [22] | Fair | Low | Low | Low | Unclear | Low | Low | Low |
| Desmots et al. [41] | Good | Low | Low | Low | Low | Low | Low | Low |
| Jung et al. [19] | Good | Low | Low | Low | Low | Low | Low | Low |
| Choi et al. [35] | Good | Low | Low | Low | Low | Low | Low | Low |
| Bhatia et al. [12] | Good | Low | Low | Low | Low | Low | Low | Low |
| Tourasse et al. [33] | Fair | Low | Low | Low | Unclear | Low | Low | Low |

Colour representation: green indicates low risk of bias and yellow indicates unclear risk of bias.

### 3.3. Meta-Analysis

In order to assess the effect of SWE parameters ($E_{max}$, $E_{mean}$, $E_{min}$, and $E_{sd}$) in diagnosing lymph node diseases, individual meta-analysis was conducted on each diagnostic setting (Figures 2–5).
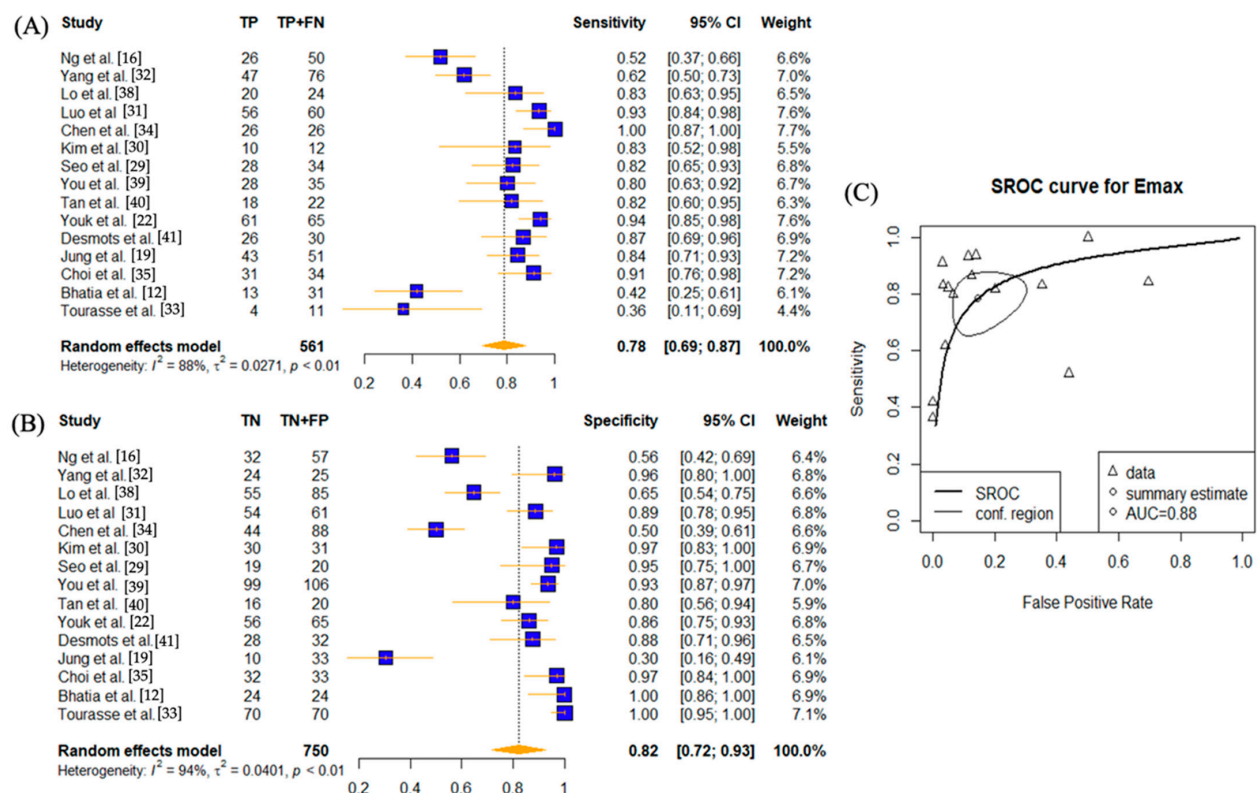


**Figure 2.** Sensitivity and specificity forest plots and overall accuracy results of $E_{max}$. (**A–C**) Reported sensitivity and specificity values for $E_{max}$ values per selected study with AUC value on SROC curve for analysis of $E_{max}$. Forest plots for pooled sensitivities and specificities are displayed as diamonds in the graphs for $E_{max}$ (**A,B**). The SROC curve indicates the summary estimates in circles ((**C**) for $E_{max}$). Triangles represent included study with dotted lines representing the confidence interval and solid line for the SROC. AUC value is displayed (in the legend). $E_{max}$—maximum tissue stiffness SWE parameter; AUC—area under the curve; SROC—summary receiver operating characteristic.
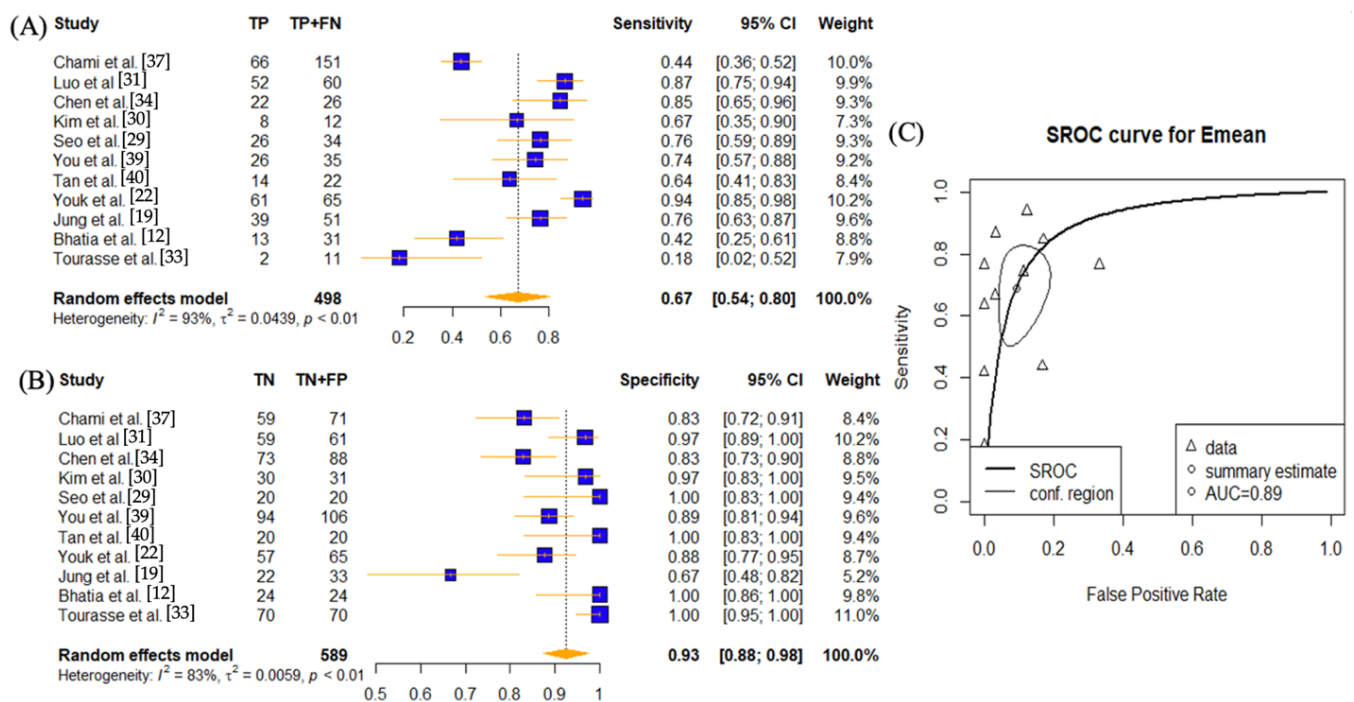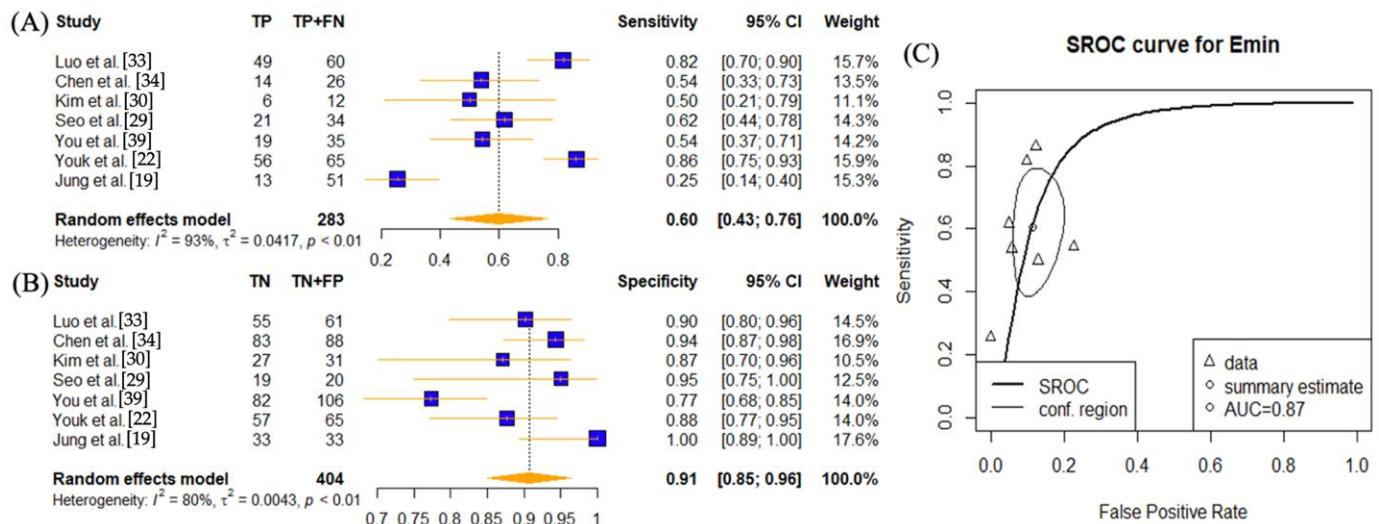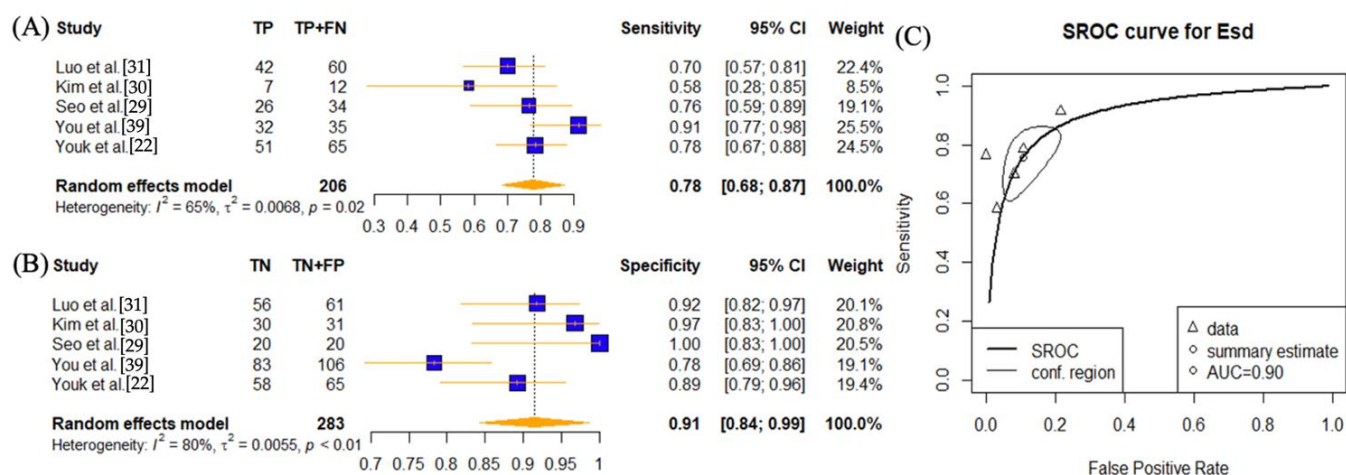
**Figure 3.** Sensitivity and specificity forest plots and overall accuracy results of $E_{mean}$. ((**A–C**) Reported sensitivity and specificity values for $E_{mean}$ values per selected study with AUC value on SROC curve for the analysis of $E_{mean}$. Forest plots for pooled sensitivities and specificities are displayed as diamonds in the graphs for $E_{mean}$ (**A,B**). The SROC curve indicates the summary estimates in circles ((**C**) for $E_{mean}$). Triangles represent included study with dotted lines representing the confidence interval and solid line for the SROC. AUC value is displayed (in the legend). $E_{mean}$—average tissue stiffness SWE parameter; AUC—area under the curve; SROC—summary receiver operating characteristic.



**Figure 4.** Sensitivity and specificity forest plots and overall accuracy results of $E_{min}$. ((**A–C**) Reported sensitivity and specificity values for $E_{min}$ values per selected study with AUC value on SROC curve for the analysis of $E_{min}$. Forest plots for pooled sensitivities and specificities are displayed as diamonds in the graphs for $E_{min}$ (**A,B**). The SROC curve indicates the summary estimates in circles ((**C**) for $E_{min}$). Triangles represent included study with dotted lines representing the confidence interval and solid line for the SROC. AUC value is displayed (in the legend). $E_{min}$—minimum tissue stiffness SWE parameter; AUC—area under the curve; SROC—summary receiver operating characteristic.

**Figure 5.** Sensitivity and specificity forest plots and overall accuracy results of $E_{sd}$. ((**A**–**C**) Reported sensitivity and specificity values for $E_{sd}$ values per selected study with AUC value on SROC curve for the analysis of $E_{sd}$. Forest plots for pooled sensitivities and specificities are displayed as diamonds in the graphs for $E_{sd}$ ((**A**,**B**). The SROC curve indicates the summary estimates in circles ((**C**) for $E_{sd}$). Triangles represent included study with dotted lines representing the confidence interval and solid line for the SROC. AUC value is displayed (in the legend). $E_{sd}$—tissue stiffness standard deviation SWE parameter; AUC—area under the curve; SROC—summary receiver operating characteristic.

Fifteen studies have investigated the use of $E_{max}$ setting [12,16,19,22,29–35,38–41] (Figure 2). The sensitivity was 0.78 (95% CI: 0.69–0.87) and specificity was 0.82 (95% CI: 0.72–0.93) The AUC value was 0.88. Again, high heterogeneities presented for both sensitivity and specificity ($p < 0.01$) across all studies.

Eleven studies have investigated the use of the $E_{mean}$ setting [12,19,22,29–31,33,34,37,39,40] (Figure 3). The sensitivity was 0.67 (95% CI 0.54–0.80) and specificity was 0.93 (95% CI: 0.88–0.98) The AUC value was 0.89. High heterogeneities presented for both sensitivity and specificity ($p < 0.01$).

Seven studies have investigated the use of the $E_{min}$ setting [19,22,29–31,34,39] (Figure 4). The sensitivity was 0.60 (95% CI: 0.43–0.76) and specificity was 0.91 (95% CI: 0.85–0.96) The AUC value was 0.87. High heterogeneities presented for both sensitivity and specificity ($p < 0.01$).

Five studies investigated the use of $E_{sd}$ setting [22,29,30,39,40] (Figure 5). The sensitivity was 0.78 (95% CI: 0.68–0.87) and specificity was 0.91 (95% CI: 0.84–0.99). The AUC value was 0.90. The heterogeneity was high for specificity ($p < 0.01$) and slightly lower for sensitivity ($p = 0.02$) but still significant.

*3.4. Sub-Group Analysis*

Sub-group analysis was also conducted to compare the use of SWE in cervical and axillary LN malignancies (Figures 6 and 7). Given that $E_{max}$ was the most common SWE parameter reported in LN malignancy detection and that it was hypothesised as the parameter with a higher sensitivity in detecting cortical focal metastases in large, heterogeneous LNs [35,41], as LNs may be partially infiltrated by the tumour or have spatial heterogeneity due to tumoral necrosis [12], it was chosen as the parameter to analyse in this sub-group analysis.
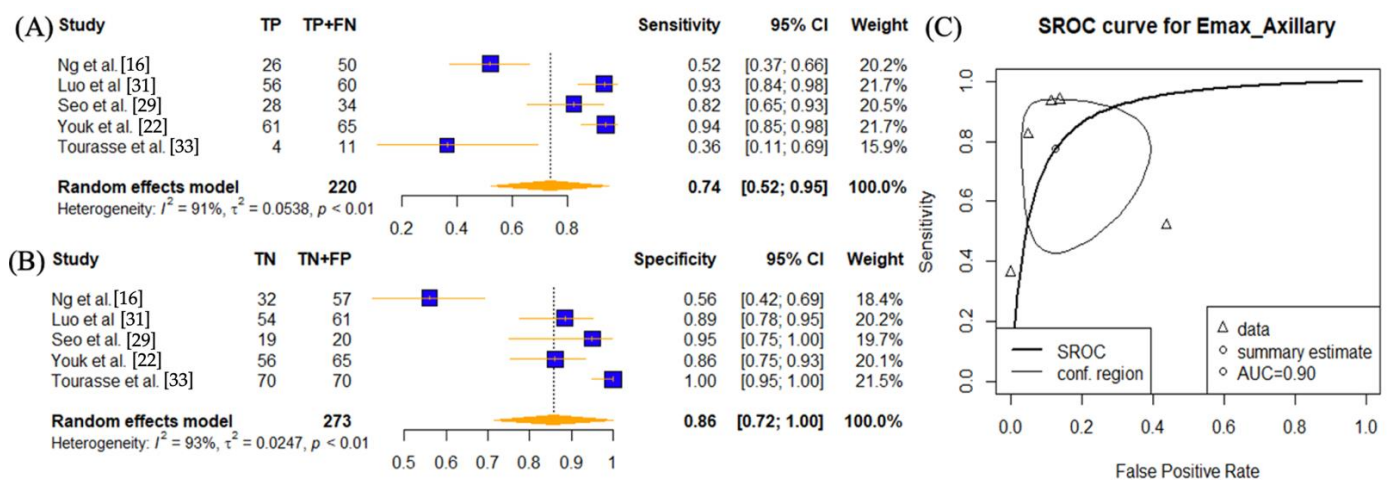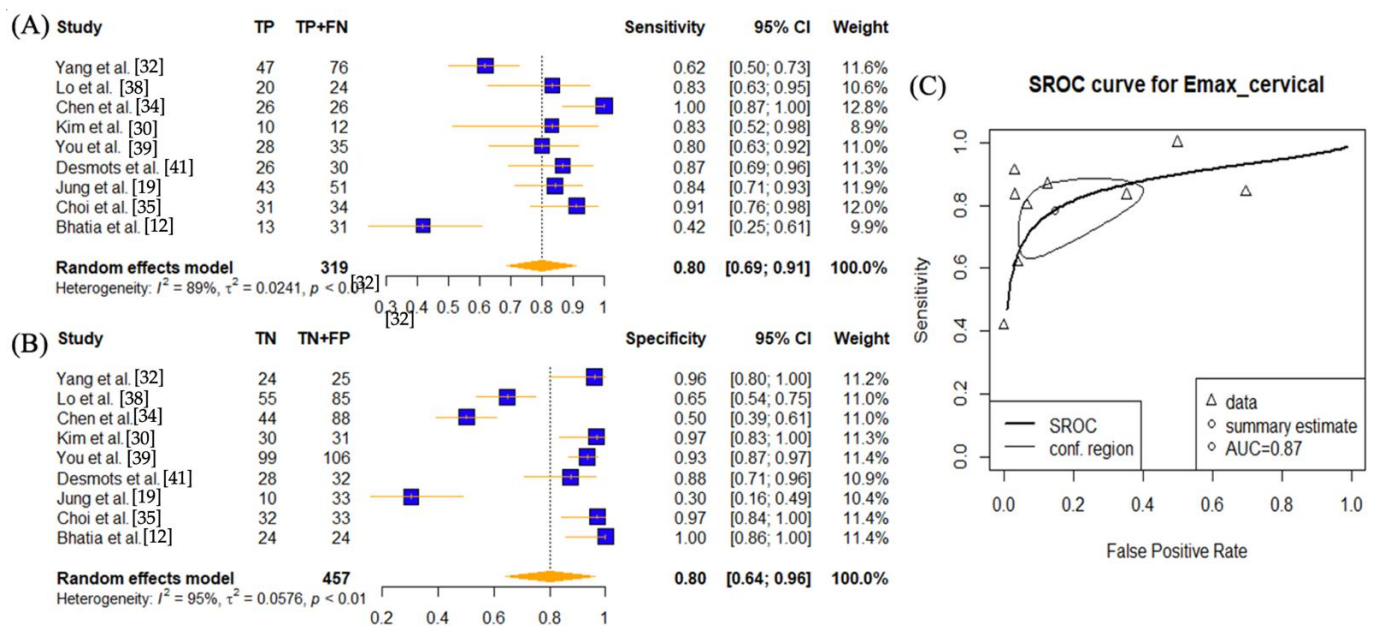
**Figure 6.** Sensitivity and specificity forest plots and overall accuracy results of $E_{max}$ in Axillary LNs. ((**A**–**C**) Reported sensitivity and specificity values for $E_{max}$ values per selected study with AUC value on SROC curve for the analysis of $E_{max}$. Forest plots for pooled sensitivities and specificities are displayed as diamonds in the graphs for $E_{max}$ (**A**,**B**). The SROC curve indicates the summary estimates in circles ((**C**) for $E_{max}$). Triangles represent included study with dotted lines representing the confidence interval and solid line for the SROC. AUC value is displayed (in the legend). $E_{max}$—maximum tissue stiffness SWE parameter; AUC—area under the curve; SROC—summary receiver operating characteristic.



**Figure 7.** Sensitivity and specificity forest plots and overall accuracy results of $E_{max}$ in cervical (including thyroid) LNs. ((**A**–**C**) Reported sensitivity and specificity values for $E_{max}$ values per selected study with AUC value on SROC curve for the analysis of $E_{max}$. Forest plots for pooled sensitivities and specificities are displayed as diamonds in the graphs for $E_{max}$ (**A**,**B**). The SROC curve indicates the summary estimates in circles ((**C**) for $E_{max}$). Triangles represent included study with dotted lines representing the confidence interval and solid line for the SROC. AUC value is displayed (in the legend). $E_{max}$—maximum tissue stiffness SWE parameter; AUC—area under the curve; SROC—summary receiver operating characteristic.

Five studies performed SWE using $E_{max}$ on axillary lymph nodes [16,22,29,31,33]. The reported pooled sensitivity was 0.74 (95% CI: 0.52–0.95) and specificity 0.86 (95% CI: 0.86–1.00) with an AUC value of 0.9. $E_{max}$ results on cervical lymph nodes, including the

thyroid, were available from nine studies [12,19,30,32,34,35,38,39,41]. The pooled sensitivity, specificity, and AUC values were 0.80 (95% CI: 0.69–0.91), 0.80 (95% CI: 0.64–0.96), and 0.87. Heterogeneities remained high ($p < 0.01$) in both sub-groups for both sensitises and specificities.

## 4. Discussion

This paper is the first systematic review and meta-analysis comparing the diagnostic accuracies of $E_{min}$, $E_{mean}$, $E_{max}$, and $E_{sd}$ SWE parameters in lymph node malignancy. The results show that the $E_{mean}$ parameter had the highest overall specificity of 0.93 (95% CI: 0.88–0.98, $I^2 = 83\%$) and both $E_{max}$ and $E_{sd}$ had the highest sensitivity of 0.78 (95% CI: 0.69–0.87, $I^2 = 88\%$ and 95% CI: 0.68–0.87, $I^2 = 65\%$). Five out of the sixteen selected studies had a complete dataset for all four SWE parameters: three indicated $E_{mean}$ as the optimal parameter with highest diagnostic accuracy [22,30,31], while two indicated $E_{max}$ as the optimal [29,39]. However, in our study among all the SWE parameters, $E_{sd}$ had the highest AUC at 0.90, but the AUC values between SWE parameters did not differ significantly.

All selected studies were conducted in either cervical or axillary lymph nodes, and existing systematic reviews have analysed the use of elastography for both types of lymph node malignancy individually, for example cervical lymphadenopathy by Suh et al. [43] and axillary lymphadenopathy by Huang et al. and Wang et al. [44,45]. However, a mixed choice of SWE parameters was pooled in analysis [43,45], and no comparisons were made between lymph node malignancies in different anatomical positions. This allowed our study to conduct a further sub-group analysis using $E_{max}$ to compare the use of SWE in cervical and axillary LNs and found a higher diagnostic performance in axillary LNs (AUC = 0.90 vs. 0.87). Wang et al. [44] reported a similar sensitivity of 0.73 (95% CI: 0.44–0.91) but a higher specificity at and 0.94 (95% CI: 0.81–0.98) and higher AUC at 0.94 (95% CI: 0.91–0.96) of $E_{max}$ in axillary lymphadenopathy. However, despite a smaller number of included studies (n = 4), their results were likely affected by high specificity value at 89.8 (85.5–94.2) reported from one ex vivo study by Bae et al. [46], introducing bias.

Studies have [22,31,40] suggested that all four SWE parameters of $E_{max}$, $E_{mean}$, $E_{min}$, and $E_{sd}$ were significantly higher for malignant LNs than benign LNs. Additionally, quantitative SWE features had significantly higher diagnostic performance than conventional grey-scale ultrasound features. Ng et al. [16] reported that the combined use of adjuvant B-mode ultrasound and qualitative SWE provided the optimal accuracy in detecting axillary LNs metastasis in their study sample (sensitivity 71.6%, specificity 95%, AUC = 0.882) in comparison with ultrasound on its own (sensitivity 70.0%, specificity 70.2%, AUC = 0.701). Tourasse et al. and Kim et al. [30,33] both emphasised the importance of high specificity or strong predictive values over false negative concerns, stating that the current main objective of SWE was to facilitate confirmation of metastatic LN diagnosis because high specificity reduces unnecessary biopsies and other invasive or high-risk investigations and enables the selection of LNs that are more likely to be malignant to undergo SNLB or FNA regardless of conventional US findings. In contrast, the high specificity is countered by low sensitivity found by Tourasse et al. ranging from 18% to 36% for $E_{mean}$ cutoffs at 19.0–23.6 kPa and 36% to 45% for $E_{max}$ at 23.7–26.5 kPa. As a result, $E_{max}$ and $E_{sd}$ may be better choices of parameters if the clinical objective is screening, based on higher sensitivity and accuracy performance, and the optimal choice of parameter used will depend on the clinical context when more data become available.

Studies by Zhao et al. [47] and Tamaki et al. [48] have also reported results of high sensitivity (85.7% and 82.8%) accompanied by relatively low specificity (54.7% and 69.6%) using other available SWE parameter that measured shear wave speed in m/s. The optimal cut-offs of the shear wave speeds differed between groups from 6.42 m/s [47] to 1.44 m/s [48]. Shear wave speed parameters are direct measurements from elastograms and are converted into elasticity SWE parameter based on assumptions, such as constant tissue density, pure tissue elasticity and isotropy, which are generally not valid [11,24]. If we were to include these studies, this conversion would introduce inaccuracy and inconsistency

between studies because the linear array transducer was operated at a different bandwidth (4–9 MHz) and SWS measurement are known to be frequency dependent [24], hence they were not included in this meta-analysis. However, future studies should investigate the relationship between the shear wave speed S parameters and elasticity E parameters to allow more accurate conversion and data pooling. Other elasticity SWE parameters, such as $E_{ratio}$ [16,22,39], $E_{median}$ [49], were also encountered in other studies but not widely used. Studies which have carried out comparative analysis between SWE and B-mode ultrasound have shown the beneficial potential of SWE as adjunct to B-mode ultrasound in enhancing the prediction of LN status in several cancers [16,44].

SWE is a novel, non-invasive, non-radioactive imaging modality that has demonstrated greater phantom resolution, fewer stress concentration artefacts related with boundaries and elastic modulus inhomogeneities and enhanced signal-to-noise ratio (SNR) with increasing depth [13]. It is thought to be more operator-independent since shear waves are created by focused high-intensity, short-duration acoustic pulses from an ultrasonic transducer rather than freehand compression as in SE [8,18]. High reproducibility of SWE has been reported by existing data according to intraclass correlation coefficients (ICCs), with the interobserver agreement ranging from 0.66–0.80 [12,50,51] and intra-observer agreement ranging from 0.64 to 0.84 [12,51]. Furthermore, SWE can provide the absolute quantification of tissue stiffness. It represents a considerable advancement over strain elastography, which can only provide the semiquantitative estimates of relative tissue strain [12,24]. Nevertheless, there are some unresolved concerns in US elastography, such as the selection of representative ROIs and unknown manufacturer-related variability in US elastography implementation. There are also a few other practical limitations due to lack of elasticity in cysts and calcified lesions, as well as a focal convex bulge on the skin overlying the ROI, which could produce spuriously stiff elastograms [8], creating scope for future studies to explore these limitations and their impact.

Molecular imaging modalities, such as PET-CT, utilising ^{18}F FDG as a biomarker to assess metabolic activity in the LNs have limitations, which can be addressed with developments in SWE technique. Sites with physiological uptake pattern, such as in the testes, it may become impossible to differentiate intense FDG uptake by neoplastic cells from normal physiological testicular activity. The implications are testicular lymphomas are treated with the orchidectomy and combination of chemotherapy. Even after treatment, physiological uptake pattern in contralateral side may be challenging to differentiate from recurrence. Gastric lymphomas may exhibit no or variable metabolic activity and this might have implications in the detection of incidentally detected nodes in the peri-gastric region [52]. Post-treatment LN evaluation is a frequent difficulty encountered in interpretation as differentiating residual nodal uptake with FDG due to lymphoma can be very difficult to differentiate from post-treatment inflammation, co-existing infection, and sites with physiological metabolic activity [53,54]. With further research and advances in this technology, SWE might have clinical impact in the detection of lymph nodes that undergo transformation, resulting in a change in tumour type, as it might be ethically unfeasible to carry out repeated biopsies and repeated cross-sectional imaging with modalities involving the radiation burden in young patients (such as females of child-bearing age and pregnant individuals) or in patients who have contra-indication to MRI.

This study has some limitations. This study found high heterogeneity ranging from 65% to 94% (Figures 2–5) and hence results should be interpreted with caution. An array of reasons for the heterogeneity could be postulated, including study design, measurement methods, reference standard, and characteristics of each study. Five of the twelve studies chosen were retrospective, which may have contributed to selection bias [19,22,29,30,32]. For example, Yang et al. and Seo et al. performed SWE on lymph nodes that were enlarged or abnormal on US findings and thus resulted in a higher proportion of metastatic LNs, contributing to selection bias and sampling error [29,32]. Additionally, direct node-to-node correlation between SWE and surgery was not obtained in all studies [16,22,33]. Tourasse et al. had reported a 10% allowance in nodal size matching between nodes

assessed by elastography and nodes surgically excised, which could have resulted in selection errors [33]. With the exception of Choi et al. [35] and You et al. [39], where the averages were 4.5 and 3.6 nodes per patient, respectively, 1.16 lymph nodes per patient were examined on average. Since the number of removed LNs ($\geq$18 in neck dissection) in resected specimens have independent prognostic value, as documented in the pathological literature [54], the low number of LN count per patient in studies selected could manifest itself in sampling error.

This study highlighted substantial discrepancies in cut-off values ranging from 15.2 to 57 kPa for $E_{max}$, 18.4 to 30.6 kPa for $E_{mean}$, and 11.4 to 24 kPa for $E_{min}$, which likely contributed to the heterogeneity, owing to differences in the reference standards. Different gold standards carry different diagnostic accuracies in determining LN malignancy. For example, studies have suggested that CNB has higher sensitivity than FNAC (87–100% and 74–83.3%, respectively), without significant differences in specificities (96–100% and 98–100%, respectively) [55–57]. When compared with surgical biopsy, CNB showed a lower sensitivity at 90% than its specificity at 100% due to false negative cases, and an LN biopsy is recommended in cases of suspected neoplasms [58,59]. In malignancies such as lymphoma, CNB is often preferred over FNAC, mainly to preserve the tissue or nodal architecture to enable comprehensive histopathological review and diagnosis [55–57]. In head and neck squamous cell cancers, FNAC are deemed to be adequate in making a diagnosis in certain cases [58,59]. The choice of gold standard needs to be put into context of the malignancy and unique patient circumstances [60]. Though variability in the use of scan technique is the reality of clinical practice, it could make the development or translation of a new imaging technique quite challenging. Surgery, on the other hand, is less prone to the variability of measurements compared to ultrasound; however, it is not always necessary or feasible to carry out nodal dissection in all patients [60,61]. Again, standard clinical practice may influence the way new or upcoming technologies are evaluated and may further compound the variability conundrum.

Depending on the underlying diseases, such as non-Hodgkin's and Hodgkin's lymphoma, mantle cell lymphoma, chronic lymphocytic leukaemia, follicular lymphoma, and metastatic malignancy, the elastographic architecture of malignant LNs may be heterogeneous [62,63]. Studies have shown that diffuse and homogenous LN infiltration are more often seen in high-grade lymphomas, whereas focal LN infiltration is indicative of low-grade follicular lymphoma [62]. However, the knowledge of elastography in differentiating grades or types of lymphomas is still very limited. Metastatic LN or lymphoma usually show peripheral or mixed patterns of internal vascularity and are difficult to differentiate, as they could both present as a round heterogenous echoic LN with hilum loss, without definite necrotic area and showing mixed vascularity [63]. It is important to discriminate these entities as the prognosis and treatment differ, and thus advanced imaging techniques are needed to differentiate them for better evaluation and treatment. Future work could explore the elastographic differences between these various types or grades of lymphomas and metastatic LNs by initially analysing their ex vivo characteristics (matched to histology) before the validation of such studies in vivo in human subjects.

Furthermore, since varying ultrasound machines have been employed across the selected studies, the measured values of shear wave speeds may differ between different systems or vendors, in particular, the shear wave vibration and the bandwidth, which may have produced shifts in elasticity values [24], and their impacts on LN diagnosis need to be further investigated in future studies [64]. Differences in software methods used to determine relative shear wave arrival time and speeds may have further led to measurement bias and adjustments for these effects are not attainable [24]. According to the most recent EFSUMB (European Federation of Societies for Ultrasound in Medicine and Biology) guidelines, the use of US elastography has been recommended for targeting malignant LNs for FNA if multiple LNs are present [64]. The difficulty in study comparison due to the lack of standardisation in technique and a definite need to set rigorous cut-off values for each of the various elastography systems and diseases have also been described [24,64].

This could be attributed to a lack of funding [24] and research in this field, emphasising the need for the greater awareness of such technologies. As a result, these findings must be carefully interpreted, with particular attention devoted to heterogeneity issues, and prospective multicentre population-based clinical trials are required to demonstrate the diagnostic value of SWE for lymph node malignancy while assuring consistency across studies to help determine whether results are acceptable clinically.

## 5. Conclusions

In conclusion, SWE has demonstrated promise as an imaging modality in diagnosing and differentiating malignancy from benign lymph nodes. Its incorporation into standard US not only allows for a better evaluation of the target region or lymph node but might reduce the need for invasive procedures or exposure to ionising radiation without compromising on diagnostic accuracy.

**Author Contributions:** Conceptualization, S.A., Y.G. and Y.Z.; methodology, Y.G., Y.Z. and S.C.; software, Y.Z.; formal analysis, Y.G. and Y.Z.; investigation, Y.G., A.C. and S.C.; data curation, Y.G.; writing—original draft preparation, Y.G., A.C., Y.Z. and S.C.; writing—review and editing, Y.G., A.C., H.D., A.H., S.W. and S.A.; visualization, Y.G., Y.Z. and H.D.; supervision, S.A.; All authors have read and agreed to the published version of the manuscript.

**Institutional Review Board Statement:** Not applicable.

**Informed Consent Statement:** Not applicable.

**Data Availability Statement:** The data presented in this study are available on request from the corresponding author.

**Conflicts of Interest:** The authors declare no conflict of interest.

## References

1. Rosen, R.D.; Sapra, A. TNM Classification. In *StatPearls*; StatPearls Publishing LLC.: Treasure Island, FL, USA, 2022.
2. Mohseni, S.; Shojaiefard, A.; Khorgami, Z.; Alinejad, S.; Ghorbani, A.; Ghafouri, A. Peripheral lymphadenopathy: Approach and diagnostic tools. *Iran. J. Med. Sci.* **2014**, *39*, 158–170. [PubMed]
3. Kawano, S.; Kojima, M.; Higuchi, Y.; Sugimoto, M.; Ikeda, K.; Sakuyama, N.; Takahashi, S.; Hayashi, R.; Ochiai, A.; Saito, N. Assessment of elasticity of colorectal cancer tissue, clinical utility, pathological and phenotypical relevance. *Cancer Sci.* **2015**, *106*, 1232–1239. [CrossRef]
4. Ophir, J.; Céspedes, I.; Ponnekanti, H.; Yazdi, Y.; Li, X. Elastography: A quantitative method for imaging the elasticity of biological tissues. *Ultrason. Imaging* **1991**, *13*, 111–134. [CrossRef]
5. Bazemore, A.W.; Smucker, D.R. Lymphadenopathy and malignancy. *Am. Fam. Physician* **2002**, *66*, 2103–2110.
6. Na, D.G.; Lim, H.K.; Byun, H.S.; Kim, H.D.; Ko, Y.H.; Baek, J.H. Differential diagnosis of cervical lymphadenopathy: Usefulness of color Doppler sonography. *AJR Am. J. Roentgenol.* **1997**, *168*, 1311–1316. [CrossRef]
7. Ahuja, A.T.; Ying, M.; Ho, S.Y.; Antonio, G.; Lee, Y.P.; King, A.D.; Wong, K.T. Ultrasound of malignant cervical lymph nodes. *Cancer Imaging* **2008**, *8*, 48–56. [CrossRef] [PubMed]
8. Choi, Y.J.; Lee, J.H.; Baek, J.H. Ultrasound elastography for evaluation of cervical lymph nodes. *Ultrasonography* **2015**, *34*, 157–164. [CrossRef] [PubMed]
9. Leenhardt, L.; Erdogan, M.F.; Hegedus, L.; Mandel, S.J.; Paschke, R.; Rago, T.; Russ, G. European thyroid association guidelines for cervical ultrasound scan and ultrasound-guided techniques in the postoperative management of patients with thyroid cancer. *Eur. Thyroid J.* **2013**, *2*, 147–159. [CrossRef] [PubMed]
10. Vassallo, P.; Edel, G.; Roos, N.; Naguib, A.; Peters, P.E. In-vitro high-resolution ultrasonography of benign and malignant lymph nodes. A sonographic-pathologic correlation. *Investig. Radiol.* **1993**, *28*, 698–705. [CrossRef] [PubMed]
11. Bamber, J.; Cosgrove, D.; Dietrich, C.F.; Fromageau, J.; Bojunga, J.; Calliada, F.; Cantisani, V.; Correas, J.M.; D'Onofrio, M.; Drakonaki, E.E.; et al. EFSUMB guidelines and recommendations on the clinical use of ultrasound elastography. Part 1: Basic principles and technology. *Ultraschall Med.* **2013**, *34*, 169–184. [CrossRef]
12. Bhatia, K.S.S.; Cho, C.C.M.; Tong, C.S.L.; Yuen, E.H.Y.; Ahuja, A.T. Shear Wave Elasticity Imaging of Cervical Lymph Nodes. *Ultrasound Med. Biol.* **2012**, *38*, 195–201. [CrossRef]
13. Melodelima, D.; Bamber, J.C.; Duck, F.A.; Shipley, J.A. Transient elastography using impulsive ultrasound radiation force: A preliminary comparison with surface palpation elastography. *Ultrasound Med. Biol.* **2007**, *33*, 959–969. [CrossRef]

14. Hill, C.R.; Bamber, J.C. Methodology for Clinical Investigation. In *Physical Principles of Medical Ultrasonics*; John Wiley & Sons Ltd.: Chichester, UK, 2004; pp. 255–302.
15. Ophir, J.; Alam, S.K.; Garra, B.S.; Kallel, F.; Konofagou, E.E.; Krouskop, T.; Merritt, C.R.B.; Righetti, R.; Souchon, R.; Srinivasan, S.; et al. Elastography: Imaging the elastic properties of soft tissues with ultrasound. *J. Med. Ultrason.* **2002**, *29*, 155. [CrossRef] [PubMed]
16. Ng, W.L.; Omar, N.; Ab Mumin, N.; Ramli Hamid, M.T.; Vijayananthan, A.; Rahmat, K. Diagnostic Accuracy of Shear Wave Elastography as an Adjunct Tool in Detecting Axillary Lymph Nodes Metastasis. *Acad. Radiol.* **2022**, *29*, S69–S78. [CrossRef]
17. Wei, C.; Li, C.; Szewczyk-Bieda, M.; Upreti, D.; Lang, S.; Huang, Z.; Nabi, G. Performance Characteristics of Transrectal Shear Wave Elastography Imaging in the Evaluation of Clinically Localized Prostate Cancer: A Prospective Study. *J. Urol.* **2018**, *200*, 549–558. [CrossRef]
18. Li, D.-D.; Xu, H.-X.; Guo, L.-H.; Bo, X.-W.; Li, X.-L.; Wu, R.; Xu, J.-M.; Zhang, Y.-F.; Zhang, K. Combination of two-dimensional shear wave elastography with ultrasound breast imaging reporting and data system in the diagnosis of breast lesions: A new method to increase the diagnostic performance. *Eur. Radiol.* **2016**, *26*, 3290–3300. [CrossRef] [PubMed]
19. Jung, W.S.; Kim, J.-A.; Son, E.J.; Youk, J.H.; Park, C.S. Shear Wave Elastography in Evaluation of Cervical Lymph Node Metastasis of Papillary Thyroid Carcinoma: Elasticity Index as a Prognostic Implication. *Ann. Surg. Oncol.* **2015**, *22*, 111–116. [CrossRef] [PubMed]
20. Sigrist, R.M.S.; Liau, J.; Kaffas, A.E.; Chammas, M.C.; Willmann, J.K. Ultrasound Elastography: Review of Techniques and Clinical Applications. *Theranostics* **2017**, *7*, 1303–1329. [CrossRef]
21. Samir, A.E.; Dhyani, M.; Anvari, A.; Prescott, J.; Halpern, E.F.; Faquin, W.C.; Stephen, A. Shear-Wave Elastography for the Preoperative Risk Stratification of Follicular-patterned Lesions of the Thyroid: Diagnostic Accuracy and Optimal Measurement Plane. *Radiology* **2015**, *277*, 565–573. [CrossRef]
22. Youk, J.H.; Son, E.J.; Kim, J.-A.; Gweon, H.M. Pre-Operative Evaluation of Axillary Lymph Node Status in Patients with Suspected Breast Cancer Using Shear Wave Elastography. *Ultrasound Med. Biol.* **2017**, *43*, 1581–1586. [CrossRef]
23. Choi, J.J.; Kang, B.J.; Kim, S.H.; Lee, J.H.; Jeong, S.H.; Yim, H.W.; Song, B.J.; Jung, S.S. Role of sonographic elastography in the differential diagnosis of axillary lymph nodes in breast cancer. *J. Ultrasound Med.* **2011**, *30*, 429–436. [CrossRef] [PubMed]
24. Dietrich, C.F.; Bamber, J.; Berzigotti, A.; Bota, S.; Cantisani, V.; Castera, L.; Cosgrove, D.; Ferraioli, G.; Friedrich-Rust, M.; Gilja, O.H.; et al. EFSUMB Guidelines and Recommendations on the Clinical Use of Liver Ultrasound Elastography, Update 2017 (Long Version). *Ultraschall Med.* **2017**, *38*, e16–e47. [CrossRef]
25. Davis, L.C.; Baumer, T.G.; Bey, M.J.; Holsbeeck, M.V. Clinical utilization of shear wave elastography in the musculoskeletal system. *Ultrasonography* **2019**, *38*, 2–12. [CrossRef] [PubMed]
26. Sandrin, L.; Tanter, M.; Gennisson, J.; Catheline, S.; Fink, M. Shear elasticity probe for soft tissues with 1-D transient elastography. *IEEE Trans. Ultrason. Ferroelectr. Freq. Control* **2002**, *49*, 436–446. [CrossRef]
27. Bercoff, J.; Tanter, M.; Fink, M. Supersonic shear imaging: A new technique for soft tissue elasticity mapping. *IEEE Trans. Ultrason. Ferroelectr. Freq. Control* **2004**, *51*, 396–409. [CrossRef]
28. Zhou, J.; Zhan, W.; Chang, C.; Zhang, X.; Jia, Y.; Dong, Y.; Zhou, C.; Sun, J.; Grant, E.G. Breast Lesions: Evaluation with Shear Wave Elastography, with Special Emphasis on the "Stiff Rim" Sign. *Radiology* **2014**, *272*, 63–72. [CrossRef]
29. Seo, M.; Sohn, Y.-M. Differentiation of benign and metastatic axillary lymph nodes in breast cancer: Additive value of shear wave elastography to B-mode ultrasound. *Clin. Imaging* **2018**, *50*, 258–263. [CrossRef]
30. Kim, H.J.; Choi, I.H.; Jin, S.-Y.; Park, H.K.; Byun, D.W.; Suh, K.; Yoo, M.H. Efficacy of Shear-Wave Elastography for Detecting Postoperative Cervical Lymph Node Metastasis in Papillary Thyroid Carcinoma. *Int. J. Endocrinol.* **2018**, *2018*, 9382649. [CrossRef]
31. Luo, S.; Yao, G.; Hong, Z.; Zhang, S.; Wang, W.; Zhang, J.; Zhang, Y.; Wu, J.; Zhang, L.; Cheng, H.; et al. Qualitative Classification of Shear Wave Elastography for Differential Diagnosis Between Benign and Metastatic Axillary Lymph Nodes in Breast Cancer. *Front. Oncol.* **2019**, *9*, 533. [CrossRef]
32. Yang, J.-R.; Song, Y.; Jia, Y.-L.; Ruan, L.-T. Application of multimodal ultrasonography for differentiating benign and malignant cervical lymphadenopathy. *Jpn. J. Radiol.* **2021**, *39*, 938–945. [CrossRef]
33. Tourasse, C.; Dénier, J.F.; Awada, A.; Gratadour, A.-C.; Nessah-Bousquet, K.; Gay, J. Elastography in the assessment of sentinel lymph nodes prior to dissection. *Eur. J. Radiol.* **2012**, *81*, 3154–3159. [CrossRef] [PubMed]
34. Chen, B.-B.; Li, J.; Guan, Y.; Xiao, W.-W.; Zhao, C.; Lu, T.-X.; Han, F. The value of shear wave elastography in predicting for undiagnosed small cervical lymph node metastasis in nasopharyngeal carcinoma: A preliminary study. *Eur. J. Radiol.* **2018**, *103*, 19–24. [CrossRef] [PubMed]
35. Choi, Y.J.; Lee, J.H.; Lim, H.K.; Kim, S.Y.; Han, M.W.; Cho, K.J.; Baek, J.H. Quantitative shear wave elastography in the evaluation of metastatic cervical lymph nodes. *Ultrasound Med. Biol.* **2013**, *39*, 935–940. [CrossRef]
36. Page, M.J.; McKenzie, J.E.; Bossuyt, P.M.; Boutron, I.; Hoffmann, T.C.; Mulrow, C.D.; Shamseer, L.; Tetzlaff, J.M.; Akl, E.A.; Brennan, S.E.; et al. The PRISMA 2020 statement: An updated guideline for reporting systematic reviews. *BMJ* **2021**, *372*, n71. [CrossRef]
37. Chami, L.; Giron, A.; Ezziane, M.; Leblond, V.; Charlotte, F.; Pellot-Barakat, C.; Lucidarme, O. Quantitative and Qualitative Approach for Shear Wave Elastography in Superficial Lymph Nodes. *Ultrasound Med. Biol.* **2021**, *47*, 2117–2127. [CrossRef]
38. Lo, W.C.; Hsu, W.L.; Wang, C.T.; Cheng, P.W.; Liao, L.J. Incorporation of shear wave elastography into a prediction model in the assessment of cervical lymph nodes. *PLoS ONE* **2019**, *14*, e0221062. [CrossRef]

39. You, J.; Chen, J.; Xiang, F.; Song, Y.; Khamis, S.; Lu, C.; Lv, Q.; Zhang, Y.; Xie, M. The value of quantitative shear wave elastography in differentiating the cervical lymph nodes in patients with thyroid nodules. *J. Med. Ultrason.* **2018**, *45*, 251–259. [CrossRef]

40. Tan, S.; Miao, L.Y.; Cui, L.G.; Sun, P.F.; Qian, L.X. Value of Shear Wave Elastography Versus Contrast-Enhanced Sonography for Differentiating Benign and Malignant Superficial Lymphadenopathy Unexplained by Conventional Sonography. *J Ultrasound Med.* **2017**, *36*, 189–199. [CrossRef] [PubMed]

41. Desmots, F.; Fakhry, N.; Mancini, J.; Reyre, A.; Vidal, V.; Jacquier, A.; Santini, L.; Moulin, G.; Varoquaux, A. Shear Wave Elastography in Head and Neck Lymph Node Assessment: Image Quality and Diagnostic Impact Compared with B-Mode and Doppler Ultrasonography. *Ultrasound Med. Biol.* **2016**, *42*, 387–398. [CrossRef] [PubMed]

42. Whiting, P.F.; Rutjes, A.W.; Westwood, M.E.; Mallett, S.; Deeks, J.J.; Reitsma, J.B.; Leeflang, M.M.; Sterne, J.A.; Bossuyt, P.M. QUADAS-2: A revised tool for the quality assessment of diagnostic accuracy studies. *Ann. Intern. Med.* **2011**, *155*, 529–536. [CrossRef] [PubMed]

43. Suh, C.H.; Choi, Y.J.; Baek, J.H.; Lee, J.H. The diagnostic performance of shear wave elastography for malignant cervical lymph nodes: A systematic review and meta-analysis. *Eur. Radiol.* **2017**, *27*, 222–230. [CrossRef]

44. Wang, R.Y.; Zhang, Y.W.; Gao, Z.M.; Wang, X.M. Role of sonoelastography in assessment of axillary lymph nodes in breast cancer: A systematic review and meta-analysis. *Clin. Radiol.* **2020**, *75*, 320.e1–320.e7. [CrossRef] [PubMed]

45. Huang, X.-W.; Huang, Q.-X.; Huang, H.; Cheng, M.-Q.; Tong, W.-J.; Xian, M.-F.; Liang, J.-Y.; Wang, W. Diagnostic Performance of Quantitative and Qualitative Elastography for Axillary Lymph Node Metastasis in Breast Cancer: A Systematic Review and Meta-Analysis. *Front. Oncol* **2020**, *10*, 552177. [CrossRef]

46. Bae, S.J.; Park, J.T.; Park, A.Y.; Youk, J.H.; Lim, J.W.; Lee, H.W.; Lee, H.M.; Ahn, S.G.; Son, E.J.; Jeong, J. Ex Vivo Shear-Wave Elastography of Axillary Lymph Nodes to Predict Nodal Metastasis in Patients with Primary Breast Cancer. *J. Breast Cancer* **2018**, *21*, 190–196. [CrossRef] [PubMed]

47. Zhao, Q.; Sun, J.-W.; Zhou, H.; Du, L.-Y.; Wang, X.-L.; Tao, L.; Jiang, Z.-P.; Zhou, X.-L. Pre-operative Conventional Ultrasound and Sonoelastography Evaluation for Predicting Axillary Lymph Node Metastasis in Patients with Malignant Breast Lesions. *Ultrasound Med. Biol.* **2018**, *44*, 2587–2595. [CrossRef] [PubMed]

48. Tamaki, K.; Tamaki, N.; Kamada, Y.; Uehara, K.; Miyashita, M.; Sm Chan, M.; Ishida, T.; Ohuchi, N.; Sasano, H. Non-invasive evaluation of axillary lymph node status in breast cancer patients using shear wave elastography. *Tohoku J. Exp. Med.* **2013**, *231*, 211–216. [CrossRef]

49. Sun, Y.; Wang, W.; Mi, C.; Zhang, Q.; Zhang, K. Differential Diagnosis Value of Shear-Wave Elastography for Superficial Enlarged Lymph Nodes. *Front. Oncol.* **2022**, *12*, 908085. [CrossRef]

50. Cosgrove, D.O.; Berg, W.A.; Doré, C.J.; Skyba, D.M.; Henry, J.-P.; Gay, J.; Cohen-Bacrie, C.; The BE1 Study Group. Shear wave elastography for breast masses is highly reproducible. *Eur. Radiol.* **2012**, *22*, 1023–1032. [CrossRef]

51. Bhatia, K.; Tong, C.S.; Cho, C.C.; Yuen, E.H.; Lee, J.; Ahuja, A.T. Reliability of shear wave ultrasound elastography for neck lesions identified in routine clinical practice. *Ultraschall Med.* **2012**, *33*, 463–468. [CrossRef] [PubMed]

52. Cronin, C.G.; Scott, J.; Kambadakone, A.; Catalano, O.A.; Sahani, D.; Blake, M.A.; McDermott, S. Utility of positron emission tomography/CT in the evaluation of small bowel pathology. *Br. J. Radiol.* **2012**, *85*, 1211–1221. [CrossRef]

53. Metser, U.; Even-Sapir, E. Increased (18)F-fluorodeoxyglucose uptake in benign, nonphysiologic lesions found on whole-body positron emission tomography/computed tomography (PET/CT): Accumulated data from four years of experience with PET/CT. *Semin. Nucl. Med.* **2007**, *37*, 206–222. [CrossRef] [PubMed]

54. Prabhakar, H.B.; Sahani, D.V.; Fischman, A.J.; Mueller, P.R.; Blake, M.A. Bowel Hot Spots at PET-CT. *Radiographics* **2007**, *27*, 145–159. [CrossRef] [PubMed]

55. Wang, M.; He, X.; Chang, Y.; Sun, G.; Thabane, L. A sensitivity and specificity comparison of fine needle aspiration cytology and core needle biopsy in evaluation of suspicious breast lesions: A systematic review and meta-analysis. *Breast* **2017**, *31*, 157–166. [CrossRef]

56. Mahmoud, O.M.; Khedrawy, M.E.-M.; Megally, H.I.; Mohamed, M.F.; Allam, M.T. Fine-needle aspiration cytology versus core needle lymph node biopsy in axillary staging of breast cancer. *Egypt. J. Radiol. Nucl. Med.* **2022**, *53*, 219. [CrossRef]

57. Amador-Ortiz, C.; Chen, L.; Hassan, A.; Frater, J.L.; Burack, R.; Nguyen, T.T.; Kreisel, F. Combined core needle biopsy and fine-needle aspiration with ancillary studies correlate highly with traditional techniques in the diagnosis of nodal-based lymphoma. *Am. J. Clin. Pathol.* **2011**, *135*, 516–524. [CrossRef]

58. Wilkinson, A.R.; Mahore, S.D.; Maimoon, S.A. FNAC in the diagnosis of lymph node malignancies: A simple and sensitive tool. *Indian J. Med. Paediatr. Oncol.* **2012**, *33*, 21–24. [CrossRef] [PubMed]

59. Höft, S.; Muhle, C.; Brenner, W.; Sprenger, E.; Maune, S. Fine-needle aspiration cytology of the sentinel lymph node in head and neck cancer. *J. Nucl. Med.* **2002**, *43*, 1585–1590.

60. Garg, S.; Rohilla, M.; Srinivasan, R.; Bal, A.; Das, A.; Dey, P.; Gupta, N.; Gupta, P.; Rajwanshi, A. Fine-Needle Aspiration Diagnosis of Lymphoma Based on Cytomorphology Alone: How Accurate is it?—A Cyto-Histopathology Correlative Study. *J. Cytol.* **2021**, *38*, 164–170. [CrossRef]

61. Kiliçarslan, A.; Doğan, M.; Süngü, N.; Karakök, E.; Karabekmez, L.; Akyol, M.; Doğan, H.T. Can Cutting-Needle Biopsy Be an Alternative to Excisional Biopsy in Lymph Node Pathologies? *Türk Patoloji Dergisi* **2017**, *1*, 235–239. [CrossRef]

62. Wang, B.; Guo, Q.; Wang, J.-Y.; Yu, Y.; Yi, A.-J.; Cui, X.-W.; Dietrich, C.F. Ultrasound Elastography for the Evaluation of Lymph Nodes. *Front. Oncol.* **2021**, *11*, 3133. [CrossRef]

63. Chae, S.Y.; Jung, H.N.; Ryoo, I.; Suh, S. Differentiating cervical metastatic lymphadenopathy and lymphoma by shear wave elastography. *Sci. Rep.* **2019**, *9*, 12396. [CrossRef] [PubMed]

64. Săftoiu, A.; Gilja, O.H.; Sidhu, P.S.; Dietrich, C.F.; Cantisani, V.; Amy, D.; Bachmann-Nielsen, M.; Bob, F.; Bojunga, J.; Brock, M.; et al. The EFSUMB Guidelines and Recommendations for the Clinical Practice of Elastography in Non-Hepatic Applications: Update 2018. *Ultraschall Med.* **2019**, *40*, 425–453. [CrossRef] [PubMed]